

Microstructure and electrical properties of ZrO₂-doped ZnO varistor ceramics

Dong Xu^{1,2} · Kai He¹ · Lei Jiao¹ · Buhua Chen² · Shuyu Mu¹ · Wenhao Wu¹ ·
Xiujuan Sun¹ · Yongtao Yang¹

Received: 3 July 2015 / Accepted: 29 September 2015 / Published online: 1 October 2015
© Springer Science+Business Media New York 2015

Abstract The microstructure and electrical properties of ZnO varistor ceramics with different ZrO₂ content prepared by a solid reaction route and sintered at 1100 °C were investigated. The microstructures of the varistor ceramics samples were characterized by X-ray diffraction and scanning electron microscopy; the electrical properties and current–voltage (*V–I*) characteristics of the varistor ceramics were investigated by DC parameter instrument. The microstructure of the prepared samples shows a decrease in grain size of ZnO phase with the ZrO₂ content increase. ZrO₂-doped ZnO varistor ceramics exhibit comparatively vastly superior comprehensive electrical properties with addition of 0.50 mol% ZrO₂, such as the threshold voltage is 350 V/mm, the nonlinear coefficient is 25.4 and the leakage current is 2.96 μA.

1 Introduction

The ZnO varistor ceramics are extensively employed in electronic devices manufacture and especially in high voltage transmission as voltage surge protector due to its excellent nonlinear *V–I* characteristics and strong energy absorption ability [1–11]. ZrO₂, characterized by high hardness, better wearing quality and longer service life, can largely reduce the waste of material grinding. Kim et al. [12] studied microstructure and electrical properties of

ZnO varistor ceramics under different ZrO₂ content and the sintering temperature. Doping with certain ZrO₂ improved comprehensive electrical properties of ZnO varistor ceramics. Wang [13] studied voltage-sensitive and dielectric properties of Zr-doped SnO₂ ceramics. The mechanism of the decrease of SnO₂ grain size with the increase of ZrO₂ concentration was discussed.

Considering that little research works of modifying the ZnO varistor ceramics by doping with ZrO₂ have even been done, furthermore, Zr⁴⁺ ion (0.080 nm) is close to Zn²⁺ ion (0.074 nm) and doping with certain ZrO₂ is very likely to exhibit unique advantages of ZnO varistor ceramics, the present work focus on the experimental investigations of the effect of ZrO₂ doping on the microstructure and electrical properties by a solid reaction route. Effects of various ZrO₂ content doping on the microstructure and the electrical properties of the ZnO varistor ceramics were investigated and some new results were obtained, which supply some theoretical foundation for ZrO₂-doped ZnO varistor ceramics.

2 Experimental

In this paper, ZrO₂ doped ZnO varistors were prepared by the solid reaction method. The samples were labeled Z0C, Z1C, Z2C, Z3C and Z4C corresponding to the different ZrO₂ content $x = 0, 0.50, 1.00, 1.50, \text{ and } 2.00$. The accurate weighted raw material $(96.50 - x)$ mol% ZnO, 0.70 mol% Bi₂O₃, 1.00 mol% Sb₂O₃, 0.80 mol% Co₂O₃, 0.50 mol% Cr₂O₃, 0.50 mol% MnO₂, and x mol% ZrO₂ were milled in ethanol in a polyethylene jar for 5 h in planetary ball mill operated at 500 r/min using zirconia balls as the milling media. The mixture was dried at 70 °C for 24 h after adequate milling. The dried powder was

✉ Dong Xu
frank@shu.edu.cn

¹ School of Material Science and Engineering, Jiangsu University, Zhenjiang 212013, People's Republic of China

² Changzhou Ming Errui Ceramics Co., Ltd., Changzhou 213102, People's Republic of China

pilled in agate mortar with the addition of 2 wt% polyvinyl alcohol binder. The powder was uniaxially pressed into pellets of 12 mm in diameter and 2 mm in thickness. The pressed pellets were sintered in air at 1100 °C for 2 h. The heating rate is 5 °C/min and the sintered the pellets were cooled inside of furnace.

The crystal structure and microstructure characteristics were investigated by X-ray diffraction (XRD, Rigaku D/max 2200, Japan) and scanning electron microscope (SEM, FEI QUANTA 400) respectively. The density of the pellets (D) was measured geometrically [14–16].

For better conducting, the silver electrodes were placed on both surfaces of the samples. The size of electrodes was 5 mm in diameter. The voltage–current (V – I) characteristics were measured using V – I source/measure unit (CJP CJ1001, China). The nominal varistor voltages (V_N) at 0.1 mA ($V_{0.1}$ mA) and 1 mA (V_1 mA) were measured [17–22]. The threshold voltage (V_T , V/mm), which was the breakdown voltage per unit thickness of varistor ceramic, was obtained from $V_T = V_1 \text{ mA}/d$, where d was the thickness of the sample in mm. The leakage current (I_L) was measured at 0.75 V_1 mA. The nonlinear coefficient (α) was determined by the equation $\alpha = 1/\lg(V_1 \text{ mA}/V_{0.1} \text{ mA})$.

3 Results and discussion

XRD patterns of ZrO₂-doped ZnO varistor ceramics samples sintered at 1100 °C for 2 h are given in Fig. 1. The samples consist typically of three phases: ZnO phase, Bi-rich phase and Zn₇Sb₂O₁₂ spinel phase [23, 24]; ZnO is the predominant phase [25]. Throughout the studied there are no fundamental differences in the phase evolution among the samples. The diffraction peaks of ZrO₂ are not

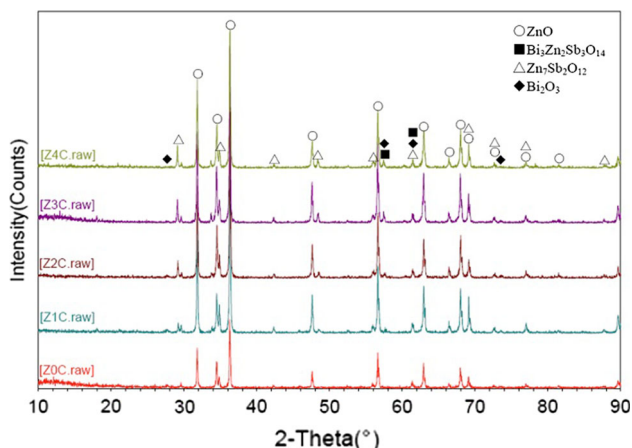


Fig. 1 XRD patterns of samples with different ZrO₂ contents sintered at 1100 °C

observed maybe because the amount of dopant is so little that they only account for a small fraction of the overall composition.

Figure 2 shows the SEM micrographs of the sample without addition of ZrO₂ and the samples doped with different amounts of ZrO₂ sintering at 1100 °C for 2 h. Those varistor ceramics samples are composed of ZnO phase, Bi-rich phase and Zn₇Sb₂O₁₂ spinel phase, as determined by XRD analysis (Fig. 1). It can be seen clearly from Fig. 2 that due to the addition of ZrO₂, the grain size of ZnO decreases greatly. Maybe when ZrO₂ doped in large quantities, a part of the ZrO₂ are dissolved in solid solution with ZnO grains. Another part of the ZrO₂ presents at the grain boundaries and strongly inhibits the growth of ZnO grain.

Figure 3 shows the relative density values of ZrO₂-doped ZnO varistor ceramics sintered at sintering temperature of 1100 °C for 2 h. The results represent that the sintered density of the varistor ceramics samples apparently increases and reaches the maximum value of 99 %. The most probable reason is that Zr⁴⁺ ion (0.080 nm) has a slightly larger radius than Zn²⁺ ion (0.074 nm). What's more, both of the electro negativities is equivalent (relative electro negativities are 1.4 and 1.6, respectively). Thus, the secondary phase tends to form solid solution, and that is, Zr is dissolved in solid solution with ZnO grains. It results in decreasing of surface energy and chemical potential and the sintering driving force increases which leads to the densification speeding up. So, density increases with the increase of the ZrO₂ content.

Figure 4 shows the leakage current of ZrO₂-doped ZnO varistor ceramics samples sintered at 1100 °C for 2 h. From Fig. 4 we can find that the leakage current increases with the increase of ZrO₂ content dramatically. The reason is that electric ZrO₂ is filled in considerably between the ZnO grains. When applying voltage, part circuits form the pathway.

The variation of the threshold voltage of ZrO₂-doped ZnO varistor ceramics samples sintered at 1100 °C for 2 h is shown in Fig. 5. It is observed that the threshold voltage firstly increases and then decreases with the increase of ZrO₂ content. It reaches the maximum value of 380 V/mm at the ZrO₂ content of 1.00 mol%.

As shown in Fig. 6, the nonlinear coefficients of ZrO₂-doped ZnO varistor ceramics samples decrease with increase in ZrO₂ content at sintering temperatures of 1100 °C for 2 h. The nonlinear coefficient as a factor of characterizing nonlinearity of a varistor, decreases with the increase of doped concentration. Its value varies from a maximum of 29.5 to a minimum of 2.1. It is seen that an increase of ZrO₂ content deteriorates the nonlinear properties.

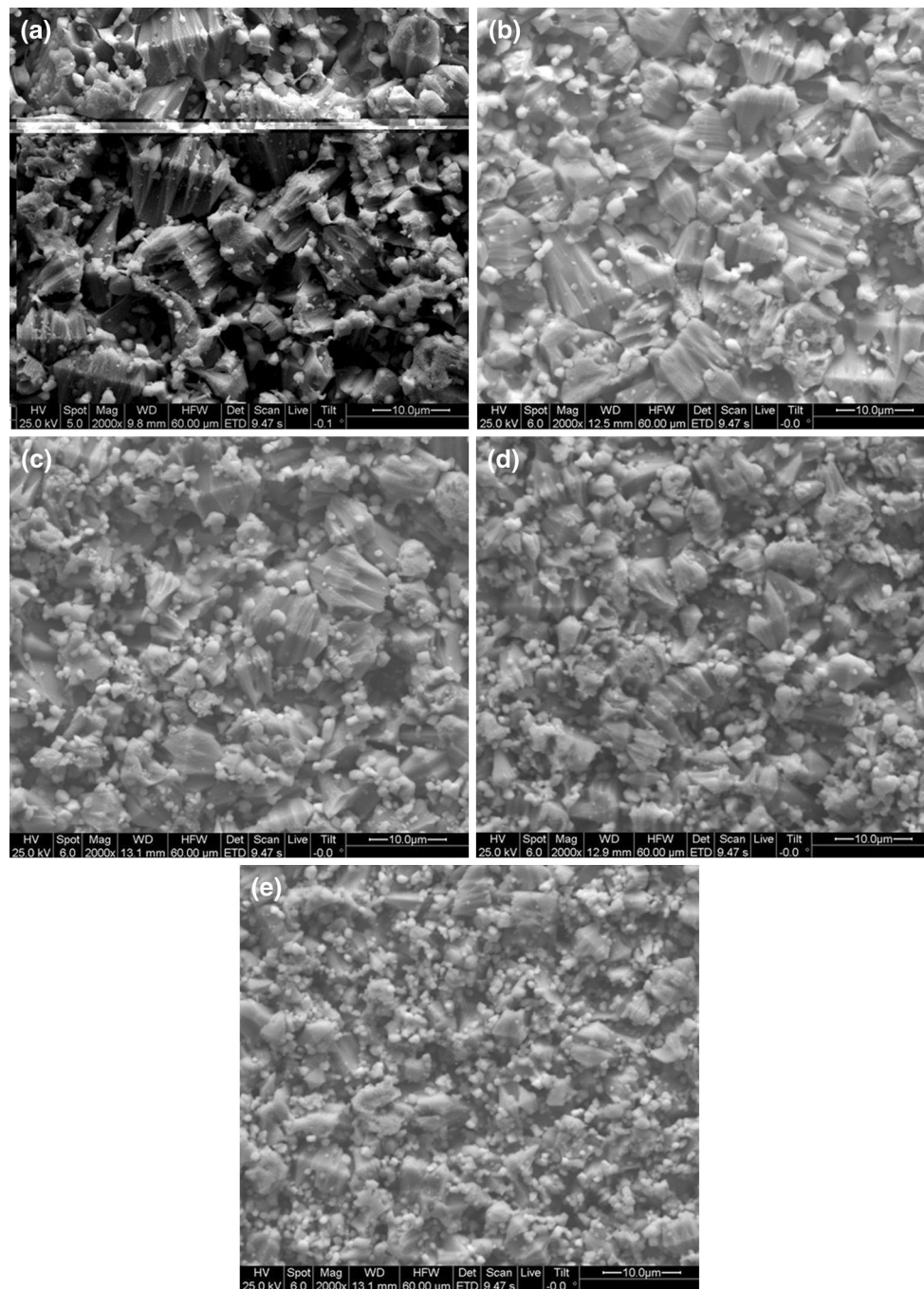


Fig. 2 SEM micrographs of different amounts of ZrO_2 doped varistor ceramics sintered at $1000\text{ }^\circ\text{C}$. **a** 0; **b** 0.5 mol%; **c** 1.0 mol%; **d** 1.5 mol%; **e** 2.0 mol%

Figure 7 presents electric field–current density (E – J) curves of ZrO_2 -doped ZnO varistor ceramics samples sintered at $1100\text{ }^\circ\text{C}$ for 2 h. The curves show that conduction characteristics are divided into two regions, namely, a linear region before the breakdown field and a nonlinear region after the breakdown field. The sharper the knee of the curves between the two regions, the better the nonlinear

property is [5, 14]. In Fig. 7, E – J curves show that potential gradient and mutation degree gradually decrease, which indicate that the nonlinear coefficients of ZrO_2 -doped ZnO varistor ceramics samples gradually decrease and it is agree with the results of Fig. 6. When doped with 2.0 mol% ZrO_2 , E – J curves are almost linear and ZnO varistor ceramics present pure resistance properties.

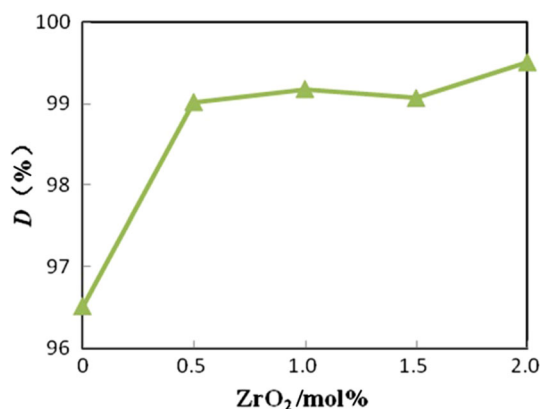


Fig. 3 Density of samples with different ZrO₂ contents sintered at 1100 °C

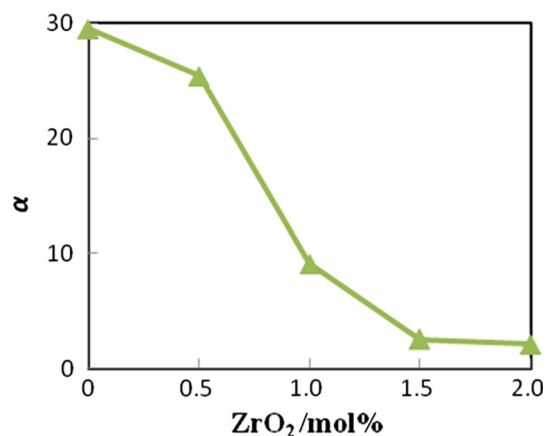


Fig. 6 Nonlinear coefficient of samples with different ZrO₂ contents sintered at 1100 °C

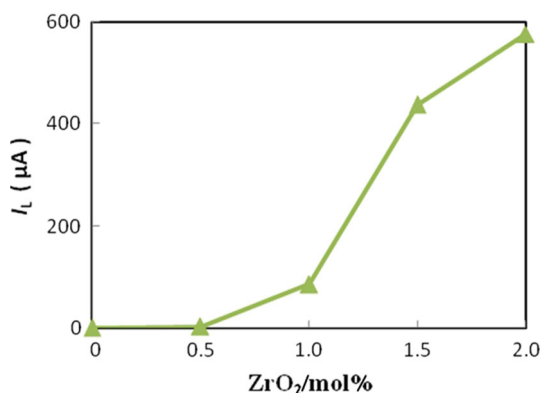


Fig. 4 Leakage current of samples with different ZrO₂ contents sintered at 1100 °C

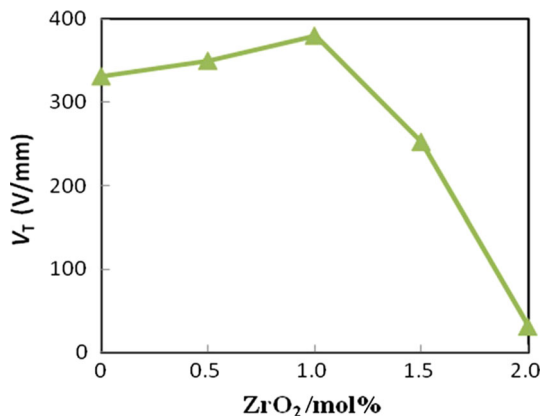


Fig. 5 Threshold voltage of samples with different ZrO₂ contents sintered at 1100 °C

4 Conclusions

The microstructure and electrical properties of ZnO varistor ceramics doped with different ZrO₂ contents were investigated. The XRD and SEM of the samples show the presence of ZrO₂. As the doping content increases, the grain size of

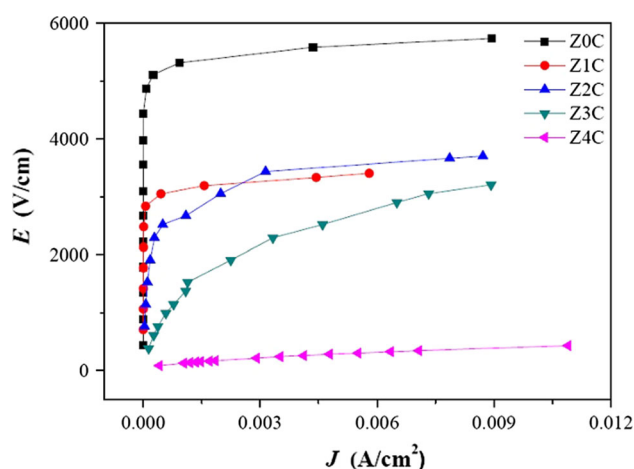


Fig. 7 E - J curves of samples with different ZrO₂ contents sintered at 1100 °C

ZnO decreases. At the same time, the nonlinear coefficient decreases. When the amount of ZrO₂ is more than 0.50 mol%, doping with ZrO₂ reduced its comprehensive electrical properties. The nonlinear V - I characteristics with the leakage current is 2.96 μ A, the threshold voltage is 350 V/mm and the nonlinear coefficient is 25.4 could be achieved when the amount of ZrO₂ is 0.50 mol% which present comparatively ideal comprehensive electrical properties of ZrO₂-doped ZnO varistor ceramics.

Acknowledgments This work was financially supported by National Natural Science Foundation of China (Grant No. 51572113), Cooperative Innovation Foundation of Jiangsu Province (BY2015064-04), Jiangsu Government Scholarship for Overseas Studies (JS-2013-097) and Changzhou science and technology Program (CQ20140006).

References

1. P. Duran, F. Capel, J. Tartaj, C. Moure, Adv. Mater. **14**(2), 137 (2002)

2. D. Xu, L.Y. Shi, Z.H. Wu, Q.D. Zhong, X.X. Wu, J. Eur. Ceram. Soc. **29**(9), 1789 (2009)
3. D. Xu, X.N. Cheng, M.S. Wang, L.Y. Shi, Adv. Mat. Res. **79–82**, 2007 (2009)
4. D. Xu, J.T. Wu, L. Jiao, H.X. Xu, P.M. Zhang, R.H. Yu, X.N. Cheng, J. Rare Earth **31**(2), 158 (2013)
5. D. Xu, X.N. Cheng, H.M. Yuan, J. Yang, Y.H. Lin, J. Alloy. Compd. **509**(38), 9312 (2011)
6. L.H. Cheng, G.R. Li, K.Y. Yuan, L. Meng, L.Y. Zheng, J. Am. Ceram. Soc. **95**(3), 1004 (2012)
7. C. Huan, F. Gang, Solid State Electron. **67**(1), 27 (2012)
8. S.A. Ansari, A. Nisar, B. Fatma, W. Khan, A.H. Naqvi, Mater. Sci. Eng. B Adv. **177**(5), 428 (2012)
9. H. Bastami, E. Taheri-Nassaj, P.F. Smet, K. Korthout, D. Poelman, J. Am. Ceram. Soc. **94**(10), 3249 (2011)
10. J.S. Park, Y.H. Han, K.H. Choi, J. Mater. Sci. Mater. El. **16**(4), 215 (2005)
11. G.H. Chen, J.L. Li, X. Chen, X.L. Kang, C.L. Yuan, J. Mater. Sci. Mater. El. **26**(4), 2389 (2015)
12. C.H. Kim, J.H. Kim, J. Eur. Ceram. Soc. **24**(8), 2537 (2004)
13. Z.J. Wang, Z.Y. Li, L. Liu, X.R. Xu, H.N. Zhang, W. Wang, W. Zheng, C. Wang, J. Am. Ceram. Soc. **93**(3), 634 (2010)
14. D. Xu, X.N. Cheng, G.P. Zhao, J.A. Yang, L.Y. Shi, Ceram. Int. **37**(3), 701 (2011)
15. Z.H. Wu, J.H. Fang, D. Xu, Q.D. Zhong, L.Y. Shi, Int. J. Min. Met. Mater. **17**(1), 86 (2010)
16. D. Xu, Q. Song, K. Zhang, H.X. Xu, Y.T. Yang, R.H. Yu, J Inorg Mater **28**(11), 1270 (2013)
17. D. Xu, D.M. Tang, L. Jiao, H.M. Yuan, G.P. Zhao, X.N. Cheng, J. Cent. South Univ. **19**(8), 2094 (2012)
18. D. Xu, D.M. Tang, L. Jiao, H.M. Yuan, G.P. Zhao, X.N. Cheng, T. Nonferr, Metal Soc. **22**(6), 1423 (2012)
19. X. Dong, H. Kai, R.H. Yu, X.J. Sun, Y.T. Yang, H.X. Xu, H.M. Yuan, J. Ma, Mater. Chem. Phys. **153**, 229 (2015)
20. H. Kai, L. Yun, R.H. Yu, J.P. Qi, X.J. Sun, Y.T. Yang, H.X. Xu, J. Ma, D. Xu, Mater. Res. Bull. **69**, 98 (2015)
21. D. Xu, C. Zhang, Y.H. Lin, L. Jiao, H.M. Yuan, G.P. Zhao, X.N. Cheng, J. Alloy. Compd. **522**, 157 (2012)
22. D. Xu, C. Zhang, X.N. Cheng, Y.E. Fan, T. Yang, H.M. Yuan, Adv. Mater. Res Switz. **197–198**, 302 (2011)
23. I.O. Ozer, E. Suvaci, S. Bernik, Acta Mater. **58**(12), 4126 (2010)
24. L. Saint Macary, M.L. Kahn, C. Estournes, P. Fau, D. Tremouilles, M. Baffleur, P. Renaud, B. Chaudret, Adv. Funct. Mater. **19**(11), 1775 (2009)
25. J.L. He, J. Liu, J. Hu, W.C. Long, Mater. Lett. **65**(17–18), 2595 (2011)